Space Weather

RESEARCH ARTICLE
10.1029/2020SW002600

One-Day Forecasting of Global TEC Using a Novel Deep Learning Model

Sujin Lee[1], **Eun-Young Ji**[1], **Yong-Jae Moon**[1,2], **and Eunsu Park**[1]

[1]Department of Astronomy and Space Science, College of Applied Science, Kyung Hee University, Yongin, South Korea, [2]School of Space Research, Kyung Hee University, Yongin, South Korea

Key Points:

- We make a global total electron content (TEC) 1-day forecasting using a deep learning model based on conditional generative adversarial networks
- Our model shows better performance than 1-day Center for Orbit Determination in Europe prediction model during the solar maximum and solar minimum periods
- We successfully apply our model to the forecast of global TEC maps using only previous TEC data

Correspondence to:
Y.-J. Moon,
moonyj@khu.ac.kr

Citation:
Lee, S., Ji, E.-Y., Moon, Y.-J., & Park, E. (2021). One-day forecasting of global TEC using a novel deep learning model. *Space Weather*, *19*, e2020SW002600. https://doi.org/10.1029/2020SW002600

Received 3 AUG 2020
Accepted 5 DEC 2020

Abstract In this study, we make a global total electron content (TEC) forecasting using a novel deep learning method, which is based on conditional generative adversarial networks. For training, we use the International GNSS Service (IGS) TEC maps from 2003 to 2012 with 2-h time cadence. Our model has two input images (IGS TEC map and 1-day difference map between the present day and the previous day) and one output image (1-day future map). The model is tested with two data sets: solar maximum period (2013–2014) and solar minimum period (2017–2018). Then, we compare the results of our model with those of 1-day Center for Orbit Determination in Europe (CODE) prediction model. Our major results can be summarized as follows. First, we successfully apply our model to the forecast of global TEC maps. Second, our model well predicts daily TEC maps with 1 day in advance using only previous TEC maps. The averaged root mean square error, bias, and standard deviation between AI-generated and IGS TEC maps are 2.74 TECU, −0.32 TECU, and 2.59 TECU, respectively. Third, our model generates some peak structures around equatorial regions. Fourth, our model shows better performance than 1-day CODE prediction model during both solar maximum and minimum periods. Fifth, another model with additional input data Kp index gives a slight improvement of the results. Our study shows that our deep learning model based on an image translation method will be effective for forecasting of future images using previous data.

Plain Language Summary The main causes of ionospheric disturbance are solar activity and geomagnetic activity. The total electron content (TEC) is one of the important parameters of ionosphere and it can be used to investigate ionospheric disturbances. We develop a global TEC 1-day forecasting model using a novel deep learning method. For training, we use the International GNSS Service TEC maps from 2003 to 2012 which include both solar maximum and minimum periods. Our model successfully forecasts the global TEC maps 1 day in advance.

1. Introduction

The total electron content (TEC) is the total number of electrons along a path between a radio transmitter and a receiver. The unit of TEC (TECU) is defined as 10^{16} electrons/m^2, and 1 TECU corresponds to a 0.163 m range delay on L1 frequency. TEC is used as one of the major parameters in space weather and an indicator of ionospheric disturbance. The accurate measurement of TEC provides us with useful information on satellite communications, navigation, national defense, and aviation.

The International Global Navigation Satellite Systems (GNSS) Service (IGS) TEC maps are calculated based on measured observational data at more than 380 IGS stations. They have been used as a reference data for comparison together with JASON satellite data (e.g., Hernández-Pajares, 2004; Jee et al., 2010; Ji et al., 2016; M. Li et al., 2018; Wang et al., 2018). These data have been made by the Ionosphere Working Group of the International GNSS Service (Iono-WG) since 1998 (Feltens & Schaer, 1998), which are currently four IGS Ionosphere Associate Analysis Centers (IAACs): the Center for Orbit Determination in Europe (CODE), the Jet Propulsion Laboratory (JPL), the European Space Operations Center of European Space Agency (ESA/ESOC), and the Polytechnical University of Catalonia (UPC). IGS produces a rapid TEC and final TEC. Rapid TEC has a latency of less than 24 h, but its accuracy is about 10%–15% lower than the final TEC (Hernández-Pajares, 2004). The final TEC maps are more reliable and accurate than the individual IAACs maps and internal consistency of all IGS products (Feltens, 2003; Hernández-Pajares et al., 2009). However, it has a latency of ~11 days.

During the last few decades, global TEC forecasting models have been developed. For example, the UPC developed a global TEC prediction model, which is based on the discrete cosine transform and linear regression module (García-Rigo et al., 2011). The model predicts a global TEC map 2 days in advance. The Space Weather Application Center Ionosphere (SWACI) provide a global TEC forecasting model 1-h in advance (Jakowski et al., 2011). Their model is based on Neustrelitz TEC model, which is a polynomial consisting of linear terms. The CODE developed the global TEC prediction models, which are based on the extrapolation of spherical harmonic expansion referring to a solar-geomagnetic frame. They have 1-day and 2 days predictions of global TEC data (Schaer, 1999). Currently, these models provide global TEC forecasts on their web site. The data is obtained from the following website: UPC and CODE (ftp://cddis.nasa.gov/gnss/products/ionex/), SWACI (https://swaciweb.dlr.de/). In view of forecasting method, these approaches mostly are based on extrapolation methods or models with a physical concept (Feltens, 2003; Hernández-Pajares et al., 2009; Z. Li et al., 2015; Mannucci et al., 1993).

Recently, many studies based on deep learning, a subset of machine learning based on artificial neural networks, have been conducted in various fields. One of deep learning algorithms, Pix2Pix is a general solution for image-to-image translation problems (Isola et al., 2017). It consists of a conditional generative adversarial networks (cGAN) and a deep convolutional generative adversarial network (DCGAN). The cGAN is an improvement model of the generation model called GAN, which attaches condition to the generator and discriminator (Mirza & Osindero, 2014). DCGAN is a deep convolution added to the generative adversarial networks (GAN), which extracts the characteristics of image and make an image similar to the input image (Radford et al., 2015).

There have been several attempts to translate images using Pix2Pix model in the field of astronomy and space science. Kim et al. (2019) successfully generated solar magnetograms from Solar Dynamics Observatory (SDO)/Atmospheric Imaging Assembly (AIA) images. Then they applied the model to STEREO/Extreme UltraViolet Imager (EUVI) 304-Å images to produce farside solar magnetograms. Park et al. (2019) successfully generated solar ultraviolet (UV) and extreme UV (EUV) images from solar magnetograms. Ji et al. (2020) developed an improved IRI model by applying this method to translation from IRI TEC maps to IGS TEC maps. These studies demonstrate that such an image translation method can be successfully applied to scientific research.

The global TEC forecasting models using deep learning also show good accuracies. For example, Perez (2019) presented a global TEC forecast model based on a multilayer perceptron. The model used six input parameters such as solar flux, Kp index, day of year, time of day, longitude, and latitude. This model can predict the global TEC 1 day or more days ahead using predicted solar flux and Kp data. Cesaroni et al. (2020) developed a global TEC forecast model based on a nonlinear autoregressive network with exogenous inputs (NARX), which is characterized by its great power to analyze nonlinear time series data. Their model used the NeQuick2 model (Nave et al., 2008) parameters and an effective sunspot number R12 calculated with NARX. They showed that the model well predicts global TEC maps during the five selected geomagnetic storms. These models used TEC data with additional parameters (solar and geomagnetic activity index) as input data.

In this paper, we develop a global TEC map forecasting model using a novel deep learning method with conditional GAN, which has been successfully applied to different kinds of image translations. Our model is 1-day prediction model which is proper for the application of image translation deep learning models. We train our model using only the IGS final TEC maps (hereafter called IGS TEC map) without additional data such as solar and geomagnetic activity index. Then, we evaluate the results of our model using several metrics and compare them with 1-day CODE prediction model. This paper is organized as follows. The data are described in Section 2. The method is explained in Section 3. Results are presented in Section 4. A brief summary and conclusion are given in Section 5.

2. Data

The IGS TEC data are obtained from the NASA's Crustal Dynamics Data Information System (CDDIS) website (ftp://cddis.nasa.gov/gnss/products/ionex/). It has a resolution 5° × 2.5° in the geographic longitude and latitude (73 by 71). We perform the data preprocessing as follows: (1) we remove the overlapping values

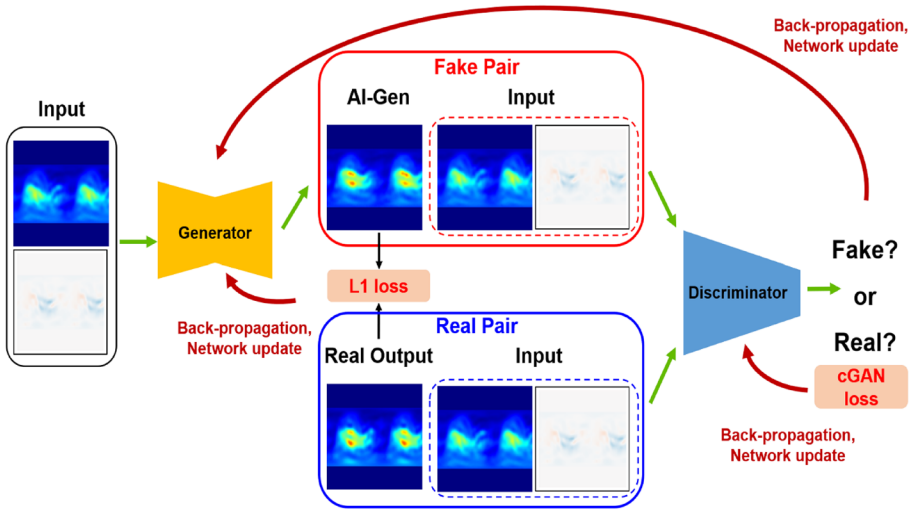

Figure 1. The architecture of our model.

on the dateline so that we make 72 by 71 images, (2) we make them 128 by 128 images for computation by adding proper padding data (same data for left and right sides, and zero values for upper and lower sides). We also make the difference TEC maps, which are the difference between the present day IGS TEC maps and the previous day data. We use the daily IGS TEC maps and 1-day difference maps as input data of our model. Output data are 1-day future maps. For training, we use the 2-h resolution TEC maps from 2003 to 2012 (43,800 images) covering solar maximum and minimum. For test, we use two data sets: solar maximum period (8,736 images) from 2013 to 2014 and solar minimum period (8,736 images) from 2017 to 2018.

3. Method

Figure 1 shows the main structure of our model. The model consists of two networks: one is a generator and the other is the discriminator. The purpose of the generator is to produce fake images similar to the output images. The purpose of the discriminator is to distinguish between real images and fake images. To train our model, we use three objectives (loss) function. The function of L_1 is expressed as:

$$L_1(G) = E_{x,y}\left(\| y - G(x) \|\right), \tag{1}$$

where G is the generator, x, y, and $G(x)$ are input, target, and output by generator, respectively. The role of this objective is to minimize the error which is the absolute value differences between the target and output by generator. The function of L_{cGAN} is expressed as:

$$L_{\text{cGAN}}(G,D) = E_{x,y}\left[\log D(x,y)\right] + E_x\left[\log\left(1 - D(x,G(x))\right)\right], \tag{2}$$

where D is the discriminator. $D(x,y)$ is the discriminator's estimation of the probability that the real pair is real. $D(x,G(x))$ is the discriminator's estimation of the probability that the fake pair is real. D calculates the probability that the image pair belongs to 0 (fake pair) or 1 (real pair). D tries to maximize the objective while the G tries to minimize it. As a result, D and G play a min-max game. Our final objective (G^*) is expressed as:

$$G^* = \arg\min_G \max_D L_{\text{cGAN}}(G,D) + \lambda L_1(G), \tag{3}$$

where λ is the relative weight of L_{cGAN} loss and L_1 loss. In this study, we use 100 for the relative weight as Isola et al. (2017) used. We initialize the weights as follows: Convolution layers and Convolution-Transpose layers using a normal distribution with 0.0 mean and 0.02 standard deviation, Batch-Normalization layers using a normal distribution with 1.0 mean and 0.02 standard deviation (Isola et al., 2017). We use the

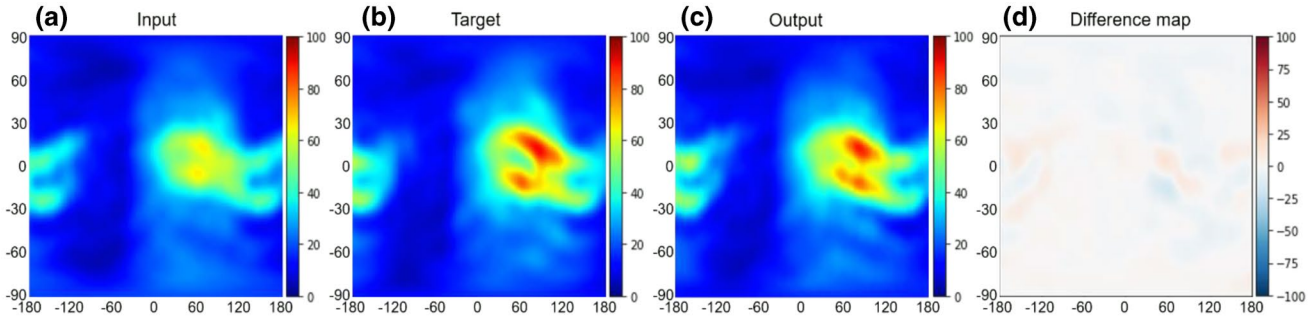

Figure 2. Comparison between IGS TEC maps and the results of our model at 02 UT on October 1, 2013. (a) input image, (b) target image (+24 h IGS TEC), (c) output image generated by our model, (d) difference map (between [b and c]).

ADAM solver as the optimizer with a learning rate of 2×10^{-4}, momentum β_1 of 0.5, and momentum β_2 of 0.999 (Isola et al., 2017; Kingma and Ba, 2014). We train our model 1,000,000 iterations for each of the solar maximum and solar minimum. Considering the CGAN loss and the statistical index, the best iteration of the solar maximum period is 800,000 iterations, and the solar minimum period is 760,000 iterations.

4. Results and Discussion

Figure 2 shows a good example among from our model, which includes an input image, the corresponding target image (+24 h IGS TEC), output image generated by our model, and the difference between the last two images at 02 UT on October 1, 2013. The Kp index when the input image was taken is 0, and the Kp index when the target image was taken is 5 which corresponds to a geomagnetic storm. The output image is well consistent with the target one, IGS TEC. Especially, our model successfully produces the peak structures in the equatorial region. The root mean square error (RMSE), bias (BIAS), and standard deviation (STD) between the output image and the target one are 2.92 TECU, −0.52 TECU, and 2.87 TECU, respectively.

Figure 3 shows a bad example among from our model, which includes an input image, the corresponding target image (+24 h IGS TEC), output image generated by our model, and the difference between the last two images at 02 UT on February 28, 2013. The Kp index when the input image was taken is 2, and the Kp index when the target image was taken is 5. The results of our model does not well generate peak structures in the equatorial region. The RMSE, BIAS, and STD between the output image and the target one are 4.43 TECU, −1.69 TECU, and 4.09 TECU, respectively.

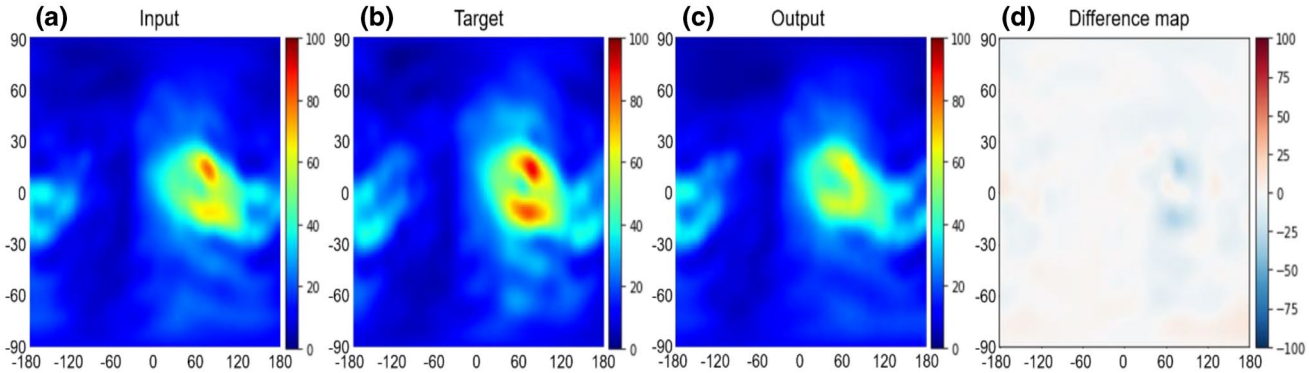

Figure 3. Comparison between IGS TEC maps and the results of our model at 02 UT on February 28, 2013. (a) input image, (b) target image (+24 h IGS TEC), (c) output image generated by our model, (d) difference map (between [b and c]).

Table 1
The Average RMSE, BIAS, and STD Values Between Forecasting Models (Ours and 1-Day CODE) and the IGS TEC During the Test Periods

	Our model—IGS TEC			1-day CODE—IGS TEC		
	RMSE	BIAS	STD	RMSE	BIAS	STD
All test data	2.74	−0.32	2.59	3.04	−0.78	2.81
Solar maximum	3.72	−0.46	3.52	4.12	−0.75	3.91
Solar minimum	1.74	−0.17	1.66	1.95	−0.81	1.72

Even though the Kp values at the target time in Figures 2 and 3 are the same, the prediction accuracy is somewhat different. We examine the temporal variations of Kp index for two cases. The first case shows that Kp decreases and then increases, and the second case shows its steady increase. The performance of a deep learning model is largely affected by the training data. In the training data, there are many cases showing the trend of change in the Kp index that increases and decreases or decreases and increases for 3 days. On the other hand, there are not many cases where Kp index continues to increase or decrease for 3 days. Therefore, the first case is much more common than the second case, which means that the model can reproduce the first pattern better than the second.

We compare our results with those of 1-day CODE prediction model. CODE is one of the IAAC and is making global TEC prediction using GNSS data. Li et al. (2018) showed that the predicted global ionosphere maps (GIM) generated at CODE are better performance than those generated at UPC and ESA. For this study, we use the 1-day CODE predicted TEC values taken from the NASA's Crustal Dynamics Data Information System (CDDIS) website (ftp://cddis.nasa.gov/gnss/products/ionex/).

Table 1 shows the averaged RMSE, BIAS, and STD between output TEC maps generated by our model and IGS TEC ones as well as between 1-day CODE predicted TEC and IGS TEC ones. We consider three test data sets: all test data (2013–2014 and 2017–2018), solar maximum period (2013–2014), and solar minimum period (2017–2018). Table 1 shows that the results of our model are better than those of the 1-day CODE prediction model for all test data. The results of our model are also better than those of 1-day CODE prediction model not only during both solar maximum period and solar minimum period.

TEC has regular changes in diurnal, seasonal, annual, 27-day, and solar cycle variations (Liu & Chen, 2009). Figure 4 shows the monthly averaged RMSE, BIAS, and STD between output TEC maps generated by our model and IGS TEC ones as well as between 1-day CODE predicted TEC and IGS TEC ones. Figure 4 shows that all our results are better than those of CODE 1-day prediction model except for two data points, which were taken in March and April 2014. These results may be related to the period of training data. In March and April 2014, solar activity is the most active during the solar cycle 24. Our training data has been included since 2003 so that our model has not been well trained for the most active case of solar cycle.

Considering the geomagnetic activity affecting the ionosphere, we make another model with additional input data, Kp index. We compare two models, one is Model A without Kp index and the other is Model B with Kp index. Table 2 shows the averaged RMSE and BIAS between output TEC maps generated by model A and B and IGS TEC ones. We consider three test data sets: all test data (2013–2014 and 2017–2018), solar maximum period (2013–2014), and solar minimum period (2017–2018). Table 2 shows that the results of Model B are slightly better than those of the Model A for all test data. As shown in the results, Model B is better. But it is noted that the Kp index used for Model B is not provided in real time. One may wonder why Model A is not bad even though we did not use Kp data. We guess that our input data (2 days TEC) already contain the effects of solar and geomagnetic activity. We expect that Model B can be used by using preliminary Kp data in the future.

5. Conclusion

In this paper, we have developed a global TEC 1-day forecasting model using deep learning based on cGAN. For training, we use the IGS TEC maps from 2003 to 2012 covering solar maximum and minimum. The model is tested with two data sets: solar maximum period (2013–2014) and solar minimum period (2017–2018).

Our major results are as follows. First, we successfully apply our deep learning model to the forecast of global TEC maps. Second, our model well predicts daily TEC maps using only previous TEC maps, without additional data such as solar and geomagnetic activity index. The averaged RMSE, BIAS, and STD between output TEC maps generated by our model and IGS TEC ones are 2.74 TECU, −0.32 TECU, and 2.59 TECU, respectively. Third, our model generates some peak structures in the equatorial regions, but not all equatorial anomalies are well predicted. Fourth, in view of the three metrics (RMSE, BIAS, and STD), the results of

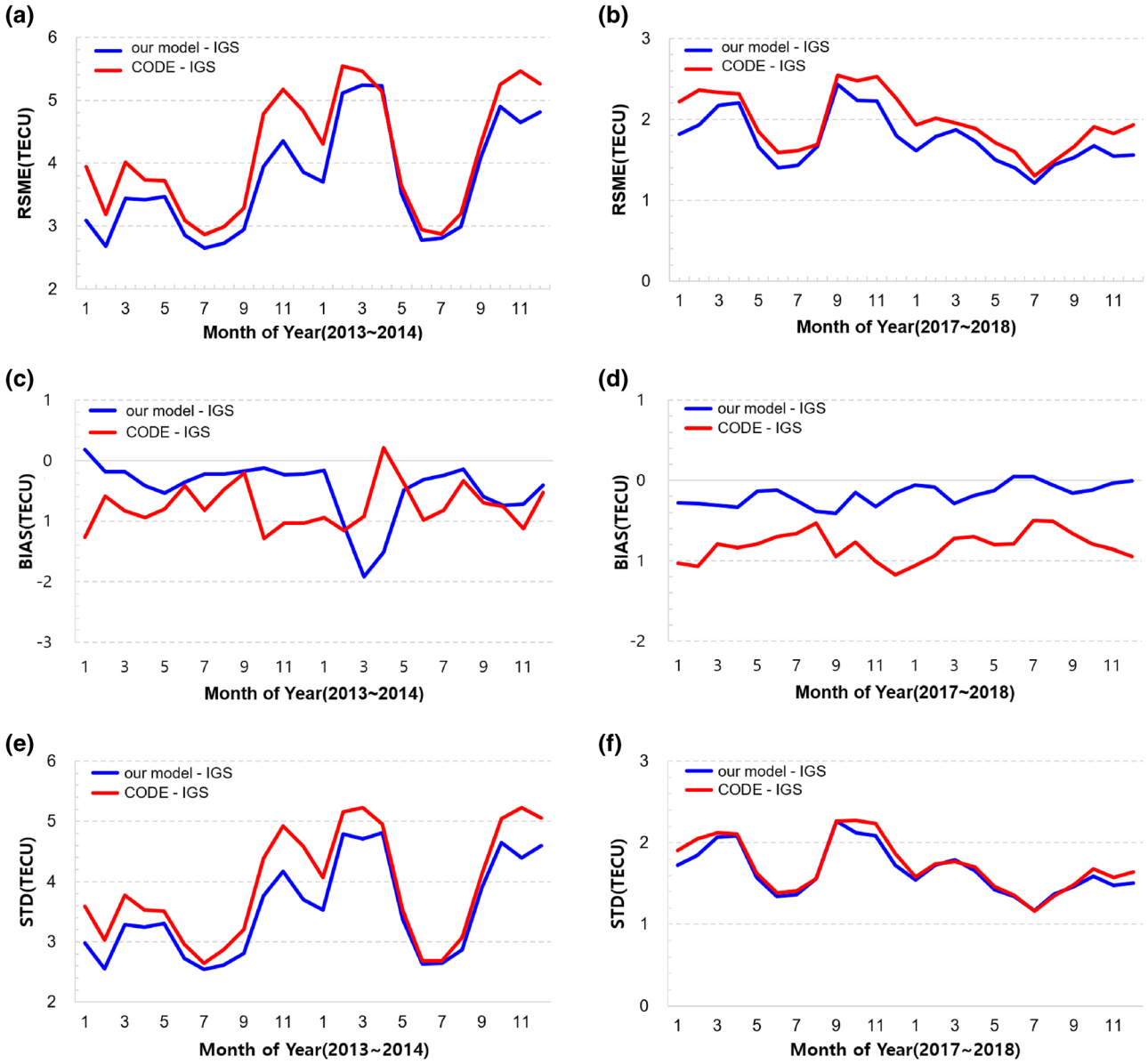

Figure 4. The monthly averaged RMSE, BIAS, and STD values between forecasting models (ours and 1-day CODE) and the IGS TEC during the test periods. (a) RMSE (solar maximum), (b) RMSE (solar minimum), (c) BIAS (solar maximum), (d) BIAS (solar minimum), (e) STD (solar maximum), (f) STD (solar minimum).

Table 2
The Average RMSE and BIAS Values Between Forecasting Models (Models A and B) and the IGS TEC During the Test Periods

	Model A		Model B	
	RMSE	BIAS	RMSE	BIAS
All test data	2.74	−0.32	2.68	−0.02
Solar maximum	3.72	−0.46	3.63	−0.08
Solar minimum	1.74	−0.17	1.72	0.03

our model are better than those of 1-day CODE prediction model during both solar maximum and solar minimum periods. Fifth, another model with additional input data Kp index gives a slight improvement of the results.

Our study demonstrates that our deep learning model based on an image translation method will be effective for forecasting future images using previous data. This method could be applied to the forecasting of images in other scientific fields. It is difficult to forecast IGS TEC maps in real time using our model since they have a latency of 11 days. Recently, Ji et al. (2020) developed an improved version of IRI TEC maps, which is called DeepIRI, by deep learning. This model can generate a global TEC

map in near real time if input parameters of IRI are properly predicted. We hope that our global model will be able to predicted in near real time with DeepIRI properly forecasted.

Data Availability Statement

The IGS TEC and CODE 1-day prediction data were obtained from the NASA's Crustal Dynamics Data Information System (CDDIS) website (ftp://cddis.nasa.gov/gnss/products/ionex/).

Acknowledgments
This work was supported by the BK21 plus program through the National Research Foundation (NRF) funded by the Ministry of Education of Korea, the Basic Science Research Program through the NRF funded by the Ministry of Education (NRF-2019R1A2C1002634, NRF-2020R1C1C1003892), the Korea Astronomy and Space Science Institute (KASI) under the R&D program "Study on the Determination of Coronal Physical Quantities using Solar Multi-wavelength Images (project No. 2020-1-850-07)" supervised by the Ministry of Science and ICT, and Institute for Information & Communications Technology Promotion (IITP) grant funded by the Korea government (MSIP) (2018-0-01422, Study on analysis and prediction technique of solar flares).

References

Cesaroni, C., Spogli, L., Aragon-Angel, A., Fiocca, M., Dear, V., De Franceschi, G., &(2020). Neural network based model for global Total Electron Content forecasting. *Journal of Space Weather and Space Climate*, *10*, 11. https://doi.org/10.1051/swsc/2020013

Feltens, J. (2003). The activities of the Ionosphere Working Group of the International GPS Service (IGS). *GPS Solutions*, *7*, 41–46. https://doi.org/10.1007/s10291-003-0051-9

Feltens, J., & Schaer, S. (1998). IGS products for the ionosphere, IGS position paper. In proceedings of the 1998 IGS Analysis Center Workshop, 225–232.

Garcia-Rigo, A., Monte, E., Hernandez-Pajares, M., Juan, J. M., Sanz, J., Aragon-Angel, A., &(2011). Global prediction of the vertical total electron content of the ionosphere based on GPS data. *Radio Science*, *46*, 1–3. https://doi.org/10.1029/2010RS004643

Hernández-Pajares, M. (2004). *IGS Ionosphere WG Status Report: Performance of IGS Ionosphere TEC Maps-Position Paper*. IGS Workshop, Barcelona, Spain.

Hernández-Pajares, M., Juan, J. M., Sanz, J., Orus, R., Garcia-Rigo, A., Feltens, J., et al. (2009). The IGS VTEC maps: A reliable source of ionospheric information since 1998. *Journal of Geodesy*, *83*, 263–275. https://doi.org/10.1007/s00190-008-0266-1

Isola, P., Zhou, J. Y., Zhou, T., & Efros, A. A. (2017). Image-to-image translation with conditional adversarial networks. In *Proceedings of the IEEE Conference on Computer Vision and Pattern Recognition*, 1125–1134.

Jakowski, N., Mayer, C., Hoque, M. M., & Wilken, V. (2011). Total electron content models and their use in ionosphere monitoring. *Radio Science*, *46*, 1–11. https://doi.org/10.1029/2010RS004620

Jee, G., Lee, H. B., Kim, Y. H., Chung, J. K., & Cho, J. (2010). Assessment of GPS global ionosphere maps (GIM) by comparison between CODE GIM and TOPEX/Jason TEC data: Ionospheric perspective. *Journal of Geophysical Research*, *115*, A10319. https://doi.org/10.1029/2010JA015432

Ji, E. Y., Jee, G., & Lee, C. (2016). Comparison of IRI-2012 with JASON-1 TEC and incoherent scatter radar observations during the 2008–2009 solar minimum period. *Journal of Atmospheric and Solar-Terrestrial Physics*, *146*, 81–88. https://doi.org/10.1016/j.jastp.2016.05.010

Ji, E. Y., Moon, Y. -J., & Park, E. (2020). Improvement of IRI global TEC maps by deep learning based on conditional Generative Adversarial Networks. *Space Weather*, *18*, e2019SW002411. https://doi.org/10.1029/2019SW002411

Kim, T., Park, E., Lee, H., Moon, Y.-J., Bae, S.-H., Lim, D., et al. (2019). Solar farside magnetograms from deep learning analysis of STEREO/EUVI data. *Nature Astronomy*, *3*, 397–400. https://doi.org/10.1038/s41550-019-0711-5

Kingma, D. P., & Ba, J. (2014). Adam: A method for stochastic optimization. *arXiv preprint arXiv:1412.6980*.

Li, M., Yuan, Y., Wang, N., Li, Z., & Huo, X. (2018). Performance of various predicted GNSS global ionospheric maps relative to GPS and JASON TEC data. *GPS Solutions*, *22*, 55. https://doi.org/10.1007/s10291-018-0721-2

Li, Z., Yuan, Y., Wang, N., Hernández-Pajares, M., & Huo, X. (2015). SHPTS: Towards a new method for generating precise global ionospheric TEC map based on spherical harmonic and generalized trigonometric series functions. *Journal of Geodesy*, *89*, 331–245. https://doi.org/10.1007/s00190-014-0778-9

Liu, L., & Chen, Y. (2009). Statistical analysis of solar activity variation of total electron content derived at Jet Propulsion Lavoratory from GPS observations. *Journal of Geophysical Research*, *114*, A10. https://doi.org/10.1029/2009JA014533

Mannucci, A. J., Wilson, B. D., & Edwards, C. D. (1993). A new method for monitoring the Earth's ionospheric total electron content using the GPS global network. In *Proceedings of ION GPS-93, Institute of Navigation*, Salt Lake City, UT, pp. 1323–1332.

Mirza, M., & Osindero, S. (2014). Conditional generative adversarial nets. *arXiv preprint arXiv:1411.1784*.

Nava, B., Coisson, P., & Radicella, S. M. (2008). A new version of the NeQuick ionosphere electron density model. *Journal of Atmospheric and Solar-Terrestrial Physics*, *70*, 1856–1862. https://doi.org/10.1016/j.jastp.2008.01.015

Park, E., Moon, Y.-J., Lee, J.-Y., Kim, R.-S., Lee, H., Lim, D., et al. (2019). Generation of solar UV and EUV images from SDO/HMI magnetograms by deep learning. *The Astrophysical Journal Letters*, *884*, L23. https://doi.org/10.3847/2041-8213/ab46bb

Perez, R. O. (2019). Using TensorFlow-based Neural Network to estimate GNSS single frequency ionospheric delay (IONONet). *Advances in Space Research*, *63*, 1607–1618. https://doi.org/10.1016/j.asr.2018.11.011

Radford, A., Metz, L., & Chintala, S. (2015). Unsupervised representation learning with deep convolutional generative adversarial networks. *arXiv preprint arXiv:1511.06434*.

Schaer, S. (1999). *Mapping and predicting the Earth's ionosphere using the global positioning system* (PhD thesis dissertation). Bern, Switzerland: Univ. of Bern.

Wang, C., Xin, S., Liu, X., Shi, C., & Fan, L. (2018). Prediction of global ionospheric VTEC maps using an adaptive autoregressive model. *Earth Planets and Space*, *70*, 1–14. https://doi.org/10.1186/s40623-017-0762-8